Journal of Solid State Chemistry 294 (2021) 121836

Contents lists available at ScienceDirect

Journal of Solid State Chemistry

journal homepage: www.elsevier.com/locate/jssc

Highly effective and fast removal of Congo red from wastewater with metal-organic framework Fe-MIL-88NH$_2$

Qiuping Fu [a,*], Jie Lou [a], Rongbin Zhang [a], Lei Peng [a], Shaoqi Zhou [b,c,**], Wei Yan [a], Changli Mo [a], Jun Luo [a]

[a] College of Chemistry and Materials Engineering, Guiyang University, Guiyang, 550005, China
[b] College of Resource and Environmental Engineering, Guizhou University, Guiyang, 550003, China
[c] Guizhou Academy Sciences, Guiyang, 550009, China

ARTICLE INFO

Keywords:
Metal organic framework
Congo red
Organic dyes
Adsorption

ABSTRACT

In the present investigation, the applicability of the adsorption and removal of the toxic organic dye Congo red (CR) from industrial wastewater using metal organic framework (MOFs) $Fe_3O(OH_2)_3Cl(NH_2\text{-}BDC)_3{\cdot}9.5H_2O$ (Fe-MIL-88NH$_2$) was evaluated. The influence of contact time, initial CR concentration, adsorbent dosage, ionic strength and temperature on the adsorption properties of Fe-MIL-88NH$_2$ were investigated. The Langmuir and Freundlich and Tempkin isotherm models have been used to discuss the adsorption behavior of CR on Fe-MIL-88NH$_2$. Tempkin adsorption isotherm model was found to be most suitable for the adsorption of CR. Different kinetic parameters were obtained by studying of adsorption kinetics on the basis of the pseudo-first-order, pseudo-second-order and intraparticle diffusion kinetic equations. The pseudo-second-order kinetic equations is most suitable for adsorption of CR on Fe-MIL-88NH$_2$, which indicates that the removal of CR are mainly carried out by chemical adsorption process.

1. Introduction

Now, organic dyes have been widely used in different industries, such as textile, printing, paper, coating, leather and so on [1,2]. Organic dyes are not easy to degrade. Organic dyes wastewater are directly discharged, which can cause serious pollution to the environment and serious harm to human health, such as skin allergies, mutation, teratogenicity and carcinogenic health problems [3]. In particular, aromatic dyes are more likely to degrade to toxic and carcinogenic poisons under exposure conditions [4]. Therefore, it is very important to remove the aromatic dyes from wastewaters. At present, several effective techniques, mainly include biodegradation [5], adsorption [6], oxidation [7], photo-degradation and flocculation precipitation have been used to remove dyes from wastewaters [8,9]. Among them, the adsorption method is considered as one of the most effective and reliable methods because of its low cost, simple operation and high efficiency. For the adsorption method, it is very important to select the appropriate adsorbent. A lot of works have been done to search for efficient adsorbent materials to remove dyes.

Metal-organic frameworks (MOFs) is a new type of porous crystalline material composed of metal ions and organic ligands [10,11]. MOFs has an extensive application prospects due to the unique properties such as high porosity, high specific surface area and catalytic efficiency, magnetic and electrochemical properties [12–15]. In particular, MOFs has attracted extensive research in the aspect of removing of organic dyes. For example, Zn-MOF [16], Al-MOF [17], Fe-MOF [18] and Cu-MOF [19] have been extensively studied for the adsorption and removal of organic dyes. Studies have shown that the interaction between MOFs and dyes can effectively remove organic dyes. The guest molecules have a large number of opportunities to enter the framework and interact with MOFs due to the large pores and high specific surface area of MOFs, which is conducive to the capture of target pollutants. In particular, its inherent open pore structure and abundant channels of MOFs can promote the rapid diffusion and migration of pollutants, thus ensuring short response time and fast absorption. In recent years, some new synthetic methods, such as surfactant-thermal method, have been used in the preparation of coordination polymers [20–24]. It further enriches the research of MOF materials.

* Corresponding author.
** Corresponding author. College of Resource and Environmental Engineering, Guizhou University, Guiyang, 550003, China.
E-mail address: Taochao5@163.com (Q. Fu).

https://doi.org/10.1016/j.jssc.2020.121836
Received 25 September 2020; Received in revised form 25 October 2020; Accepted 26 October 2020
Available online 27 October 2020

It has been reported that the nano-porous MOFs $Fe_3O(OH_2)_3Cl(NH_2$-BDC)$_3$·9.5H_2O (Fe-MIL-88NH_2) has been synthesized by using 2-amino-terephthalic acid as ligand [25,26]. Fe-MIL-88NH_2 is a non-toxic nano-material with high specific surface area, containing a large number of surface amino groups. Fe-MIL-88NH_2 is a promising material for removal of organic dye [27,28]. However, as far as we know, there have been no reports on Fe-MIL-88NH_2 adsorption of organic dyes Congo red (CR). In this paper, Fe-MIL-88NH_2 was synthesized by solvothermal method, and its adsorption properties on CR aqueous solution were studied. The effects of initial concentration of CR, contact time, adsorbent dosage and ionic strength on the adsorption efficiency of CR were investigated. The adsorption mechanism was further studied by discussing the adsorption isotherm, kinetic and thermodynamic characteristics.

2. Experimental section

2.1. Experimental materials and instruments

Raw materials and reagents: Ferric chloride hexahydrate ($FeCl_3$·6H_2O), 2-amino-terephthalic acid (BDC-NH_2), Congo red (CR), N,N-Dimethylformamide (DMF), all reagents and chemicals are analytically pure. Ultrapure water was made in the laboratory.

2.2. Characterization

X-ray diffraction (XRD) pattern of the as-prepared Fe-MIL-88NH_2 was characterized by using a Rigaku Ultima-IV X-ray diffractometer. Fourier transform infrared (FTIR) spectra of the as-prepared Fe-MIL-88NH_2 were characterized by Fourier transform infrared spectrometer (Shimadzu, Japan). Scanning electron microscope (SEM) images of Fe-MIL-88NH_2 were characterized by the field-emission scanning electron microscope (FESEM). The Uv–vis absorption spectra of CR solution was measured by using a BlueStarA UV–Vis spectrophotometer (LabTech, Beijing).

2.3. Preparation of metal-organic framework (Fe-MIL-88NH_2)

Fe-MIL-88NH_2 was synthesized according to the literature [26]. In detail, 0.3789 g $FeCl_3$·6H_2O and 0.2536 g BDC-NH_2 was dissolved in 15 mL DMF solution, the mixed solution was stirred for 10 min. Then the solution was sealed in 25 mL Teflon-lined autoclave for 20 h at 140 °C. The resulting samples were filtered and washed three times with DMF. The samples were dried in vacuum at 60 °C for 20 h, and the red brown powder solids were obtained. Yield: 53% (based on Ferric chloride hexahydrate).

2.4. Adsorption experiments

The adsorption experiments were carried out on CR with different initial concentrations (5–60 mg/L), different temperature (30, 40 and 50 °C). 15 mg adsorbents Fe-MIL-88NH_2 were added into 50 mL CR solution and placed inside a thermostatic bath shaker for 5–120 min. Then the supernatant of the solution was separated by centrifugation and the absorbance of the supernatant was measured by ultraviolet spectrophotometer.

The adsorption capacity (q_e) and removal rate (R) of CR were calculated by the following formula ,

$$q_e = \frac{(C_0 - C_e)V}{m}$$

$$R(\%) = \frac{C_0 - C_e}{C_0} \times 100\%$$

where, C_0 (mg/L) and C_e (mg/L) are the initial and equilibrium concentrations of CR, respectively; V (L) is the volume of CR solution; m (mg) is the mass of the adsorbent.

3. Results and discussions

3.1. Structural and morphology characterization of Fe-MIL-88NH_2

The crystal structure and phase purity of the as-prepared samples were verified by XRD pattern (Fig. S1). It can be seen from Fig. S1 that the XRD diffraction peaks of Fe-MIL-88NH_2 materials are very sharp, which indicates that the crystallinity of as-synthesized sample is high. All diffraction peaks are completely consistent with the reported Fe-MIL-88NH_2 pattern (Cambridge Crystallographic Data Center (CCDC) 647,646) [29], which indicates the successful synthesis of Fe-MIL-88NH_2. The absence of impurity peak indicates that pure phase of Fe-MIL-88NH_2 has been obtained.

FTIR spectra of Fe-MIL-88NH_2 is shown in Fig. S2. In Fig. S2, the bands at 1389 cm^{-1} and 1602 cm^{-1} are attributed to the symmetrical and asymmetrical vibration modes of the carboxyl group. The bands at 3370 cm^{-1} and 3458 cm^{-1} are attributed to the symmetrical and asymmetrical stretching vibrations of amine groups, the band at 1645 cm^{-1} correspond to the bending vibration of amine groups [30], which confirms the presence of amino groups in the as-prepared Fe-MIL-88NH_2.

Fig. 1 shows the SEM images of Fe-MIL-88NH_2. As can be seen from the figure, the as-synthesized Fe-MIL-88NH_2 crystals with the morphology of spindle structure and ununiform size, which is consistent with the report in literature [31].

3.2. Effect of initial concentration of CR and contact time on adsorption of CR

15 mg Fe-MIL-88NH_2 was added to 50 mL CR solution with different concentrations (5–60 mg/L). In order to study the effect of contact time on the adsorption efficiency, the absorbance of the remaining CR solution was measured at different time-intervals (5–120 min). Fig. 2 shows the effect of initial CR concentrations on the adsorption of Fe-MIL-88NH_2 in 0–120 min. As can be seen from the figure, the adsorption of CR on Fe-MIL-88NH_2 from CR solution with initial concentration of 5–10 mg/L reached equilibrium in 5 min. The adsorption of CR solution with initial concentration of 15–60 mg/L reached equilibrium in 60 min. The adsorption capacity of CR on Fe-MIL-88NH_2 increases rapidly with increasing time. The adsorption rate is very fast in the beginning. Due to a large number of adsorption active sites on the surface of adsorbent Fe-MIL-88NH_2, and there is a strong affinity between Fe-MIL-88NH_2 and Congo red.

The concentration of CR decreases in the solution, amount of CR adsorbed on the adsorbent increases, and the adsorption sites on the adsorbent decrease accordingly, the adsorption driving force decrease gradually. Meanwhile, the repulsion force of CR inside the adsorbent is enhanced, and the adsorption power decreases gradually, adsorption equilibrium was reached at about 120 min.

3.3. Effect of adsorbent dosage on adsorption of CR

To study the influence of Fe-MIL-88NH_2 dosage on adsorption, 5–25 mg Fe-MIL-88NH_2 were added in 40 mg/L CR solution. Fig. 3 shows the influence of Fe-MIL-88NH_2 dosage on the adsorption capacity and removal rate of CR. As can be seen from the figure, the equilibrium adsorption capacity of CR decreases with increasing of Fe-MIL-88NH_2 dosage. Due to the addition amount of Fe-MIL-88NH_2 is smaller, the amount of CR around Fe-MIL-88NH_2 per unit mass is larger, and the driving force of mass transfer is greater, which is conducive to the binding of CR on the active site of Fe-MIL-88NH_2, promoting adsorption, and increasing the equilibrium adsorption amount of CR on Fe-MIL-88NH_2. When the amount of adsorbent is large, the overcrowding adsorbent particles in the solution will lead to the overlap of adsorption binding sites, which results in the decrease of the equilibrium adsorption capacity of Congo red.

However, the removal rate of CR firstly increases with increasing of

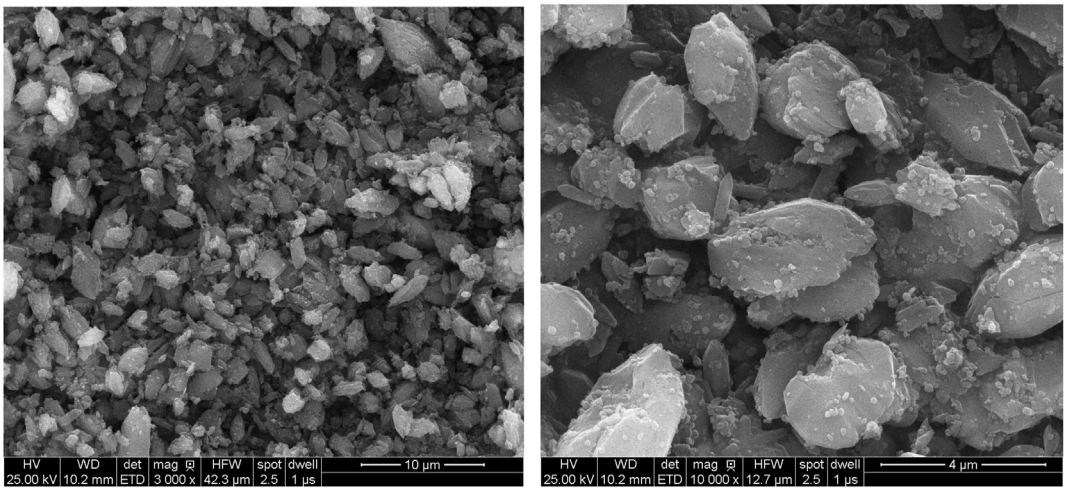

Fig. 1. SEM images of Fe-MIL-88NH$_2$.

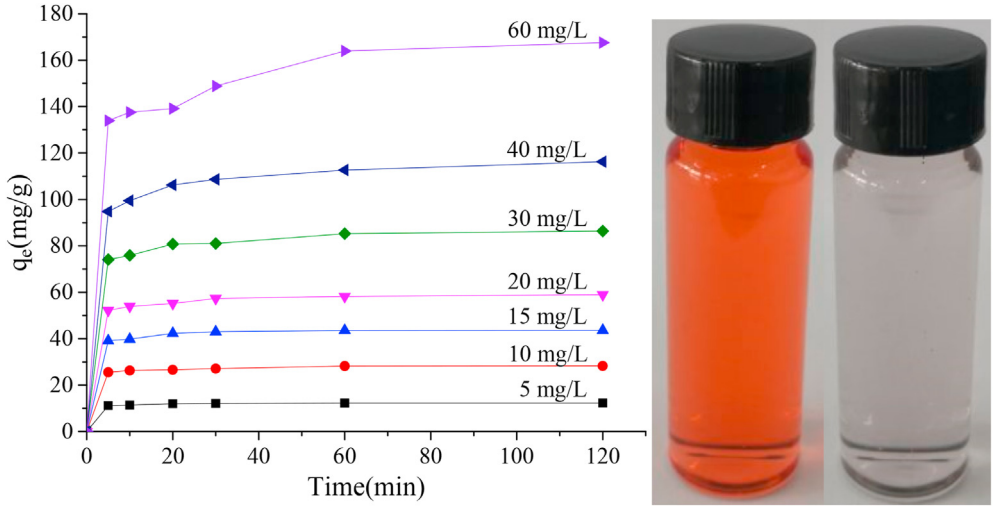

Fig. 2. Effect of contact time on removal of CR, pictures of CR solution at 40 mg/L before and after adsorption.

Fe-MIL-88NH$_2$ dosage from 5 mg to 15 mg. Due to the increase of the amount of adsorbent, the surface area and adsorption site of the adsorbent increase, which improves the removal rate of CR. When the dosage of Fe-MIL-88NH$_2$ is more than 15 mg, the removal rate of CR can reach 87.2%, and the removal rate has little change when the dosage of Fe-MIL-88NH$_2$ continues to increase. The optimum dosage of adsorbent Fe-MIL-88NH$_2$ was determined to be 15 mg by combining removal rate and actual cost.

3.4. Effect of ionic strength on adsorption of CR

The presence of salinity in the solution could affect the electrostatic and non-electrostatic interactions on the surface of adsorbent. Therefore, the effect of ionic strength on removal of CR was investigated in this paper.

15 mg Fe-MIL-88NH$_2$ were added in 40 mg/L CR solution with different concentration of NaCl. The contact time is 60 min, and the results are shown in Fig. 4. The removal rate of CR increased slightly with the concentration of NaCl increasing from 0 mol/L to 0.05 mol/L. The removal rate decreased while concentration of NaCl exceeded 0.05 mol/L. This may be due to competition between Na^+ and CR for limited number of active binding sites. Especially, the removal of CR was impeded due to the exchange reaction and competition among ions when the active binding site saturated on the surface of adsorbent [32]. On the other hand, the change of salinity may also change the activity coefficient of adsorbate, which resulting in the inhibition of the adsorption process [33].

3.5. Adsorption isotherms

The interaction between CR and adsorbent Fe-MIL-88NH$_2$ are analyzed by the Langmuir, Freundlich and Temkin isothermal adsorption models. The monolayer adsorption of dye molecules on the surface of the adsorbent was assumed by Langmuir isothermal adsorption model. And there is no interaction among the adsorbed dye molecules. The Freundlich isothermal adsorption model is based on the heterogeneous multilayer adsorption of dye molecules on the adsorbent surface. The interaction between adsorbents and dye was studied by Temkin isothermal adsorption model. The corresponding equations of Langmuir, Freundlich and Temkin isothermal adsorption models are expressed as following [34,35],

Langmuir isotherm equation. $\frac{C_e}{q_e} = \frac{1}{k_L q_m} + \frac{C_e}{q_m}$

Freundlich isotherm equation. $\ln q_e = \ln k_F + \frac{1}{n}\ln C_e$

Temkin isotherm equation. $q_e = \frac{RT}{b_T}\ln k_T + \frac{RT}{b_T}\ln c_e$ where k_L is the Langmuir adsorption constant (L/mg), and q_m is maximum adsorption capacity (mg/g). k_f is the Freundlich adsorption constant (mg/g), and n is

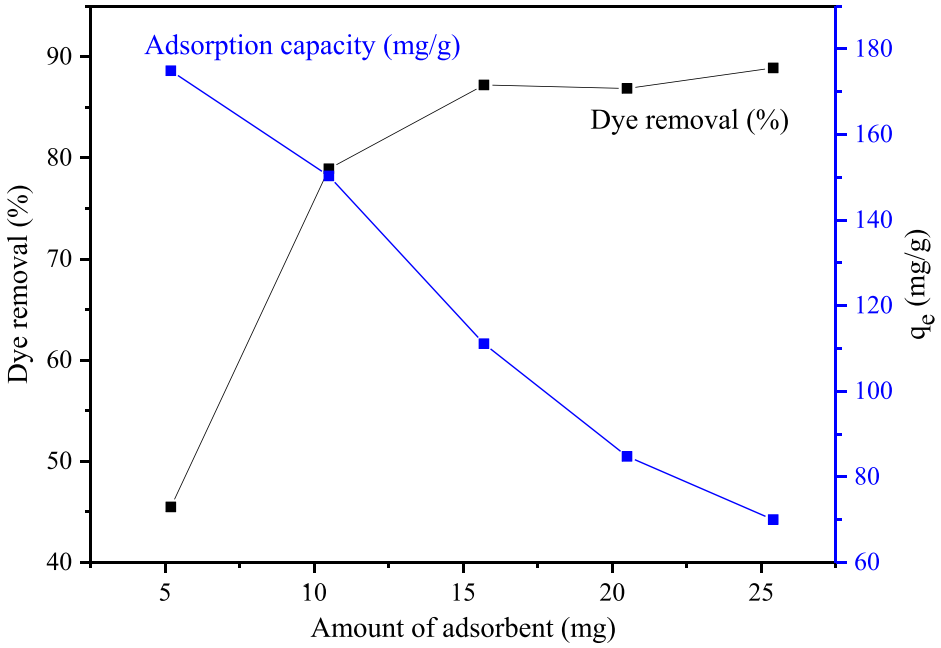

Fig. 3. Effect of adsorbent dosage on adsorption of CR.

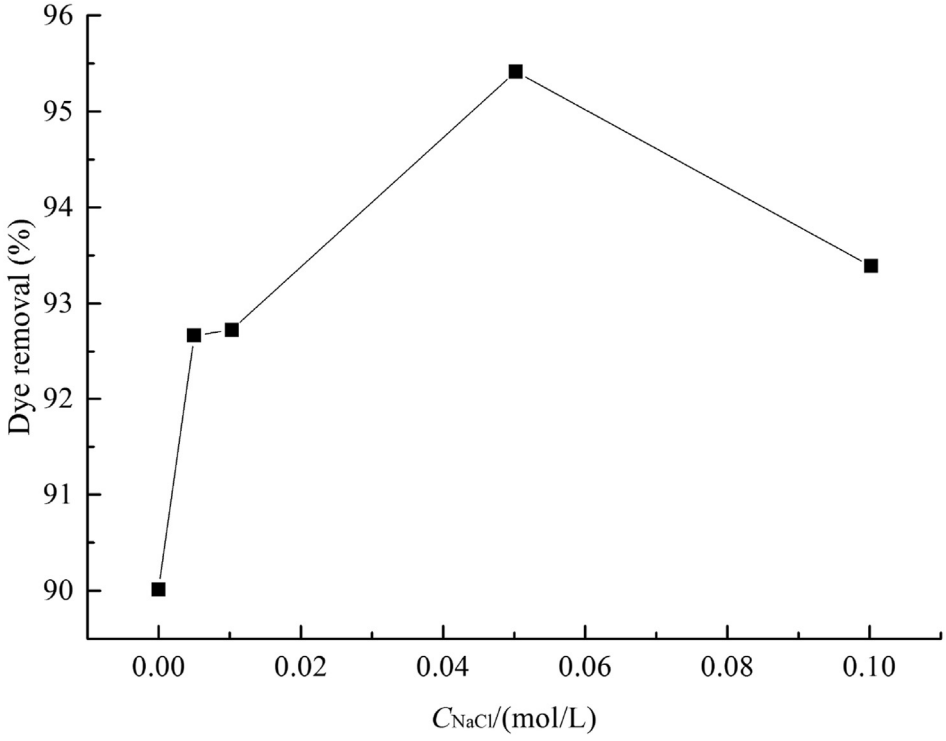

Fig. 4. Effect of ionic strength on removal of CR.

the adsorption intensity. k_T is the equilibrium binding constant (mol^{-1}), b_T is the constant of adsorption heat, R is the ideal gas state constant (8.314 J/mol/K) and T is temperature (K). Temkin adsorption isotherm indicates that non-equivalent adsorption sites exist on the surface of the adsorbent, and the adsorption of dyes firstly occurs on the adsorption site with large energy.

The linear fits of adsorption isotherm of CR on Fe-MIL-88NH_2 are shown in Fig. 5(a–c) by using three adsorption isotherm models, Langmuir, Freundlich and Temkin isotherm models. The parameters of the corresponding isothermal adsorption model are shown in Table 1. The relationship between adsorption amount (q_e) and the residual concentration of CR is shown in Fig. 5(d). The correlation coefficient (R^2) is used to confirm the optimal isothermal adsorption model. By comparing the correlation coefficient (R^2) fitted by the three models, it can be known that the adsorption process of CR on Fe-MIL-88NH_2 is more consistent with the Temkin isothermal adsorption model than other two models. The results indicate that the main adsorption sites are on the heterogeneous surface of Fe-MIL-88NH_2.

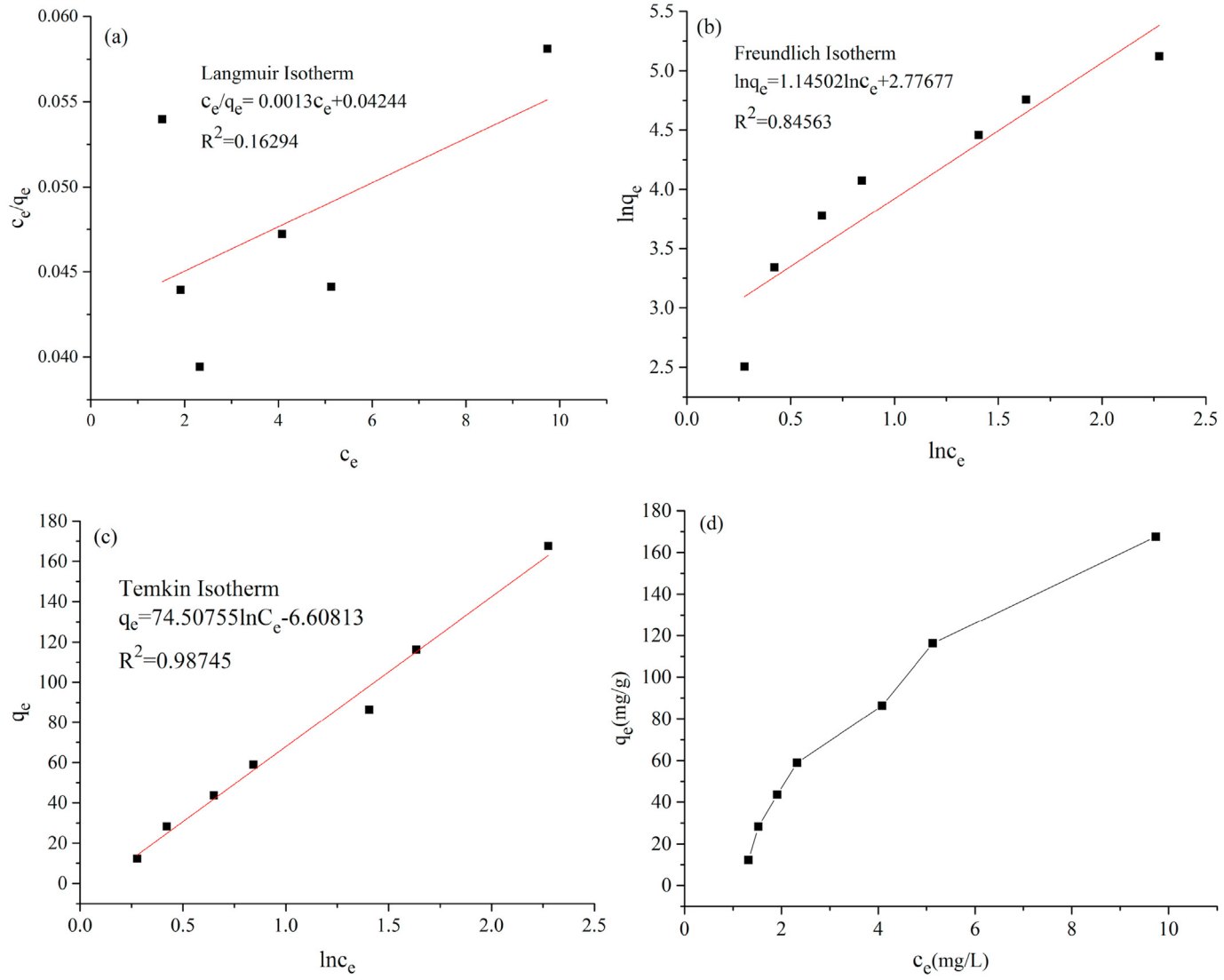

Fig. 5. Linear plot for (a) Langmuir, (b) Freundlich, (c) Temkin adsorption isotherms and (d) plot between C_e and q_e.

Table 1
Isotherm parameters for CR adsorption on Fe-MIL-88NH$_2$.

Concentration of dye (mg/L)		Q_e (mg/g)	Langmuir isotherm			Freundlich isotherm			Temkin isotherm		
Initial	C_e		q_L	k_L	R^2	n	k_f	R^2	b_T	k_T	R^2
5	1.319	12.270	769.231	0.031	0.16294	0.873	16.067	0.84563	33.811	0.915	0.98745
10	1.525	28.250									
15	1.917	43.611									
20	2.323	58.922									
30	4.080	86.401									
40	5.129	116.238									
60	9.736	167.547									

In Temkin isothermal adsorption equation, the constant adsorption heat (b_T) represents the change of adsorption energy. When $b_T < 1000$ J/mol, the adsorption of CR on Fe-MIL-88NH$_2$ is an endothermic reaction. When $b_T > 1000$ J/mol, the adsorption is an exothermic reaction [36]. In Temkin isothermal adsorption model, the b_T value is 33.811 J/mol at 303 K, which indicates that the adsorption of CR on Fe-MIL-88NH$_2$ is an endothermic reaction.

3.6. Adsorption kinetics

In order to explore the adsorption mechanism and the potential rate control steps in the adsorption process, it is necessary to study the adsorption kinetic model. The experimental dynamic curves are shown in Fig. 6. In this paper, the adsorption mechanism of CR on Fe-MIL-88NH$_2$ was studied by the pseudo-first-order kinetics and pseudo-second-order kinetics and intraparticle diffusion models. The linear equations of the three kinetic models are expressed as following [35,37],

pseudo-first-order kinetic models $\ln(q_e - q_t) = \ln q_e - k_1 t$

pseudo-second-order kinetic models $\frac{t}{q_t} = \frac{1}{k_2 q_e^2} + \frac{t}{q_e}$

intraparticle diffusion models. $q_t = k_{id} \cdot t^{0.5} + C$where, q_e (mg/g) and q_t (mg/g) are the amount of CR adsorbed at equilibrium and at time t (min), respectively. The k_1 (min^{-1}), k_2 (g/mg·min), k^{id} (mg/g·min$^{1/2}$)

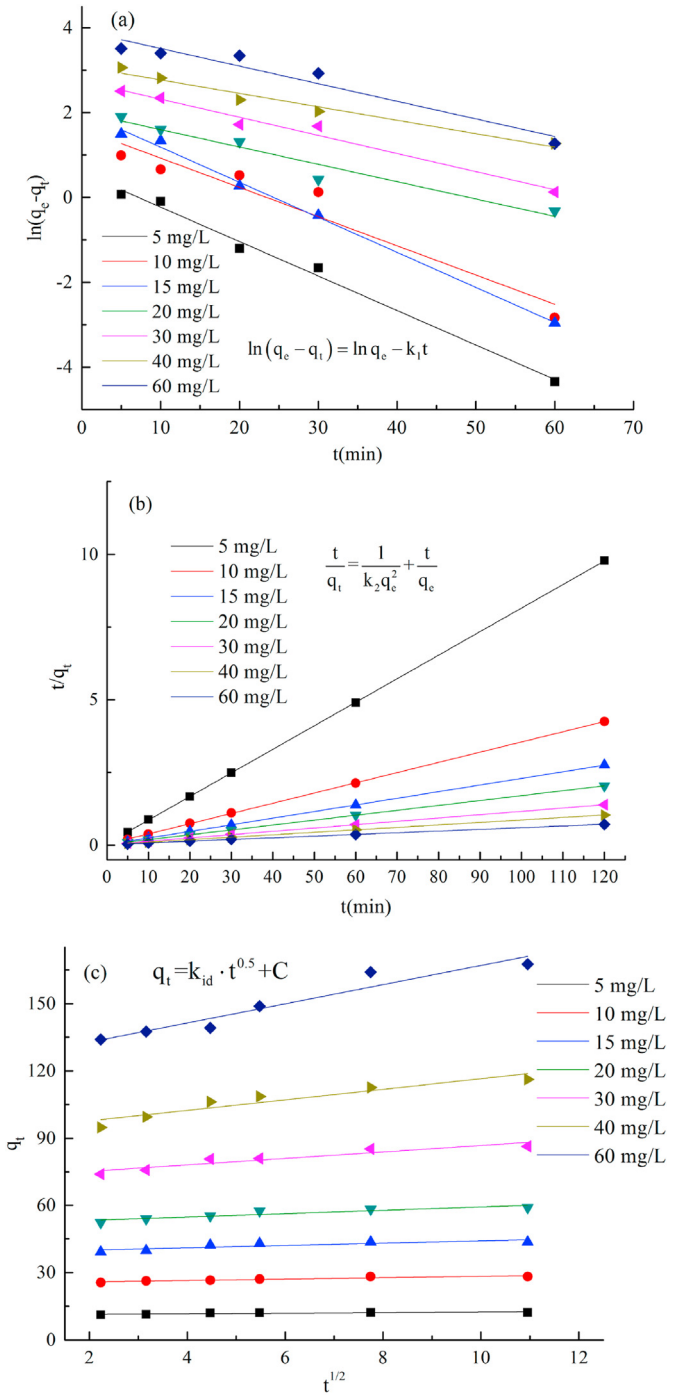

Fig. 6. Linear plot for (a) pseudo first order, (b) pseudo second order and (c) intraprticle diffusion models.

are adsorption rate constant for pseudo first order, pseudo second order and intraparticle diffusion models, respectively. The boundary layer effect is reflected by the intraparticle diffusion constant C.

Fig. 6 shows the linear fitting results of three models. The parameters of the three models are shown in Table 2. Fig. 6 and Table 2 show that the correlation coefficient (R^2) of the pseudo-second-order dynamic model is greater than 0.99, and the correlation coefficient (R^2) of the pseudo-second-order dynamic model is greater than that of the other two models. The results show that the pseudo-second-order kinetic model is more suitable for the adsorption of CR on Fe-MIL-88NH$_2$. It can be concluded that CR is mainly removed from wastewater through chemisorptions by using the Fe-MIL-88NH$_2$ as adsorbent.

3.7. Adsorption thermodynamics

Adsorption thermodynamics were used to studied the variation of adsorption capacity with temperature, which is one of the important characteristics of adsorption capacity. The study of adsorption thermodynamics plays an important role in the application of adsorption materials in practical engineering. Thermodynamic parameters such as Enthalpy change (ΔH), Entropy change (ΔS) and Gibbs free energy change (ΔG) for the adsorption of CR on Fe-MIL-88NH$_2$ can be calculated according to the following formula [35,38],

$$Kc = \frac{qe}{ce}$$

$$\Delta G = \Delta H - T\Delta S$$

$$\ln Kc = \frac{\Delta S}{R} - \frac{\Delta H}{RT}$$

where, K_c is the standard thermodynamic equilibrium constant, T is temperature (K), R (8.314 J/mol/K) is the ideal gas state constant. The values of ΔH and ΔS is calculated from the slope and intercept that provided by the plots of ln (q_e/C_e) versus 1/T.

The thermodynamic fitting curves and parameters are shown in Fig. 7 and Table 3, respectively. It can be seen from the table that the value of ΔG is negative, which indicates the feasibility and spontaneity of the adsorption process of CR on Fe-MIL-88-NH$_2$ [39]. Moreover, the absolute value of ΔG increases with increasing of temperature, which indicates that high temperatures are favorable for the adsorption process. ΔH is positive value, which indicates that the adsorption of CR on Fe-MIL-88-NH$_2$ is an endothermic process, further proves that the high temperature conditions are conducive to the adsorption process.

3.8. Reusability and selectivity of Fe-MIL-88NH$_2$

Fe-MIL-88NH$_2$ could be recovered after Congo red adsorption and reused. The used Fe-MIL-88NH$_2$ was regenerated by a simple process using ethanol as an desorption agent until the solution becomes completely clear. The specific operation is as following, 15 mg Fe-MIL-88NH$_2$ was added to 50 mL of CR dye with initial concentration of 40 mg/L for adsorption for 1 h. Then Fe-MIL-88NH$_2$ was collected and washed with ethanol for 3 times. The adsorbent was dried in an oven at 60 °C for 20 h. The above adsorption experiment was repeated after the sample was dried. The removal efficiency of CR remains above 83% after undergoing 4 cycles, which shows excellent adsorption stability of Fe-MIL-88NH$_2$.

In order to further determine the selectivity for CR, two another organic dyes: methyl orange (MO) and methylene blue (MB) are also applied in the adsorption. The adsorption capacity for MO (58.72 mg/g) and MB (15.99 mg/g) are obviously smaller than that of CR. The results show that Fe-MIL-88NH$_2$ has a certain selective adsorption for CR.

4. Conclusions

In this study, a metal-organic framework Fe-MIL-88-NH$_2$ was successfully prepared by solvothermal method. Fe-MIL-88-NH$_2$ was used as an adsorbent to remove the organic dye CR from wastewater. Effective factors on the adsorption capacity including contact time, initial concentration, adsorbent dosage, ionic strength and temperature were investigated. The results showed significant correlation between the equilibrium adsorption data and Temkin adsorption isotherm. The pseudo-first-order, pseudo-second-order and intra-particle diffusion model were used to explain the interaction between Fe-MIL-88-NH$_2$ and CR. It was found that the pseudo-second-order model was most suitable to explain the interaction between CR and Fe-MIL-88-NH$_2$. The thermodynamic parameters show that the adsorption of CR on Fe-MIL-88-

Table 2
Kinetic parameters for adsorption of CR on Fe-MIL-88NH_2.

Initial concentration (mg/L)	Pseudo-first-order model			Pseudo-second-order model			Intraparticle diffusion model		
	Q_e	K_1	R^2	Q_e	K_2	R^2	k_{id}	C	R^2
5	1.798	0.081	0.9924	12.343	0.128	0.99998	0.123	11.158	0.7232
10	7.494	0.069	0.932	28.490	0.035	0.99989	0.315	25.209	0.8888
15	5.048	0.083	0.9966	43.917	0.031	0.99998	0.513	38.983	0.7174
20	7.460	0.041	0.9497	59.382	0.016	0.99995	0.751	51.714	0.845
30	15.590	0.043	0.9774	87.413	0.007	0.99985	1.431	72.460	0.8845
40	21.988	0.032	0.9682	117.647	0.004	0.99978	2.352	93.004	0.8884
60	50.887	0.046	0.9413	171.527	0.002	0.99894	4.272	124.271	0.9262

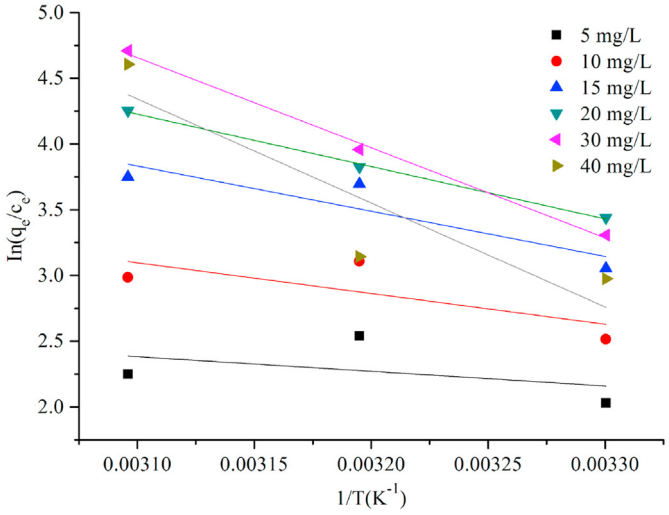

Fig. 7. Plots of $\ln q_e/C_e$ versus 1/T for CR adsorption on Fe-MIL-88-NH_2.

Table 3
Thermodynamic parameters for adsorption of CR on Fe-MIL-88-NH_2.

Dye concentration (mg/L)	ΔH (kJ/mol)	ΔS (kJ/mol/K)	ΔG (kJ/mol) at temperatures		
			303 K	313 K	323 K
5	9.238	0.048	−5.439	−5.924	−6.408
10	19.406	0.086	−6.621	−7.480	−8.339
15	28.580	0.121	−7.921	−9.125	−10.330
20	33.105	0.138	−8.639	−10.016	−11.394
30	56.962	0.215	−8.274	−10.427	−12.580
40	65.799	0.240	−6.946	−9.347	−11.748

NH_2 is a spontaneous endothermic process. The above results indicate that Fe-MIL-88-NH_2 can be used as an effective adsorbent for removing of organic pollutant CR from wastewater. The application of MOFs for dye removal/degradation is extended by the work. And Fe-MIL-88-NH_2 is a promising adsorbent for removing of organic dye CR.

CRediT authorship contribution statement

Qiuping Fu: Conceptualization, Methodology, Investigation, Writing - original draft, Funding acquisition. **Jie Lou:** Data curation. **Rongbin Zhang:** Software. **Lei Peng:** Formal analysis. **Shaoqi Zhou:** Supervision, Funding acquisition, Validation. **Wei Yan:** Writing - review & editing. **Changli Mo:** Investigation. **Jun Luo:** Project administration.

Declaration of competing interest

The authors declare that they have no known competing financial interests or personal relationships that could have appeared to influence the work reported in this paper.

Acknowledgments

This project was supported by National Key R&D Program of China (2016YFC0400702), Science and Technology Foundation of Guizhou Province (Qiankehejichu[2018]1007), Discipline and Master's Site Construction Project of Guiyang University by Guiyang City Financial Support Guiyang University (HC-2020).

Appendix A. Supplementary data

Supplementary data related to this article can be found at https://doi.org/10.1016/j.jssc.2020.121836.

References

[1] L.N. Jin, J. Ye, Y. Wang, X.Y. Qian, M.D. Dong, Fiber. Polym. 20 (2019) 2070–2077.
[2] J. Panda, J.K. Sahoo, P.K. Panda, S.N. Sahu, M. Samal, S.K. Pattanayak, R. Sahu, J. Mol. Liq. 278 (2019) 536–545.
[3] Z.N. Shi, C. Xu, H. Guan, L. Li, L. Fan, Y.X. Wang, L. Liu, Q.T. Meng, R. Zhang, Colloids Surf. A: Physicochem. Eng. Asp. 539 (2018) 382–390.
[4] X.P. Quan, Z.Q. Sun, H. Meng, Y.D. Han, J.B. Wu, J.L. Xu, Y. Xu, X. Zhang, J. Solid State Chem. 270 (2018) 231–241.
[5] S. Shanmugam, P. Ulaganathan, K. Swaminathan, S. Sadhasivam, Y.R. Wu, Int. Biodeter. Biodegr. 125 (2017) 258–268.
[6] M. Yang, Q.H. Bai, Colloid. Surface A 582 (2019) 123795.
[7] F. Ke, L.G. Qiu, J.F. Zhu, Nanoscale 6 (2014) 1596–1601.
[8] K.C. Devarayapalli, S.V. Prabhakar Vattikuti, T.V.M. Sreekanth, K.S. Yoo, P.C. Nagajyothi, J. Shim, Mater. Res. Express 6 (2019) 1150h3.
[9] G. Hitkari, S. Singh, G. Pandey, Int. J. Adv. Res. Sci., Eng. Tech. 4 (2017) 3960–3965.
[10] Y.Z. Li, G.D. Wang, H.Y. Yang, L. Hou, Y.Y. Wang, Z.H. Zhu, Inorg. Chem. Front. 7 (2020) 746–755.
[11] N. Zhao, Y. Li, J.Z. Gu, M.V. Kirillova, A.M. Kirillov, Dalton Trans. 48 (2019) 8361–8374.
[12] H. Kaur, R. Kumar, A. Kumar, V. Krishnan, R.R. Koner, Dalton Trans. 48 (2019) 915–927.
[13] Y.M. Tan, Z.Q. Sun, H. Meng, Y.D. Han, J.B. Wu, J.L. Xu, Y. Xu, X. Zhang, Powder Technol. 356 (2019) 162–169.
[14] Q.S. Zhang, X. Jiang, A.M. Kirillov, Y.W. Zhang, M.Y. Hu, W. Liu, L.Z. Yang, R. Fang, W.S. Liu, ACS Sustain. Chem. Eng. 7 (2019) 3203–3212.
[15] K. Iqbal, A. Iqbal, A.M. Kirillov, W.S. Liu, Y. Tang, Inorg. Chem. 57 (2018) 13270–13278.
[16] J. Panda, J.K. Sahoo, P.K. Panda, S.N. Sahu, M. Samal, S.K. Pattanayak, R. Sahu, 278 (2019) 536-545.
[17] R. Azhdari, S.M. Mousavi, S.A. Hashemi, S. Bahrani, S. Ramakrishna, J. Environ. Chem. Eng. 7 (2019) 103437.
[18] S.H. Tian, S. Xu, J.T. Liu, C. He, Y. Xiong, P.Y. Feng, J. Clean. Prod. 239 (2019) 117767.
[19] Y. Xu, J.J. Jin, X.L. Li, Y.D. Han, H. Meng, C.S. Song, X. Zhang, Microchim Acta 182 (2015) 2313–2320.
[20] W.W. Xiong, Q.C. Zhang, Angew. Chem. 54 (2015) 11616–11623.
[21] P. Li, F.F. Cheng, W.W. Xiong, Q.C. Zhang, Inorg. Chem. Front. 5 (2018) 2693–2708.
[22] F.F. Cheng, J.N. Zhu, M.Y. Zhao, Z.J. Ma, W.W. Xiong, J. Solid State Chem. 278 (2019) 120904.
[23] M.Y. Zhao, J.N. Zhu, P. Li, W. Li, T. Cai, F.F. Cheng, W.W. Xiong, Dalton Trans. 48 (2019) 10199–10209.
[24] Z.J. Ma, W. Li, J.M. Yu, Z.Z. Zhang, X.Q. Zhu, W.W. Xiong, X.Y. Huang, J. Solid State Chem. 285 (2020) 121248.
[25] Z.W. Jiang, Y.L. Liu, X.L. Hu, Y.F. Li, Anal. Methods 6 (2014) 5647.
[26] D.H. Xie, Y. Ma, Y. Gu, H.J. Zhou, H.M. Zhang, G.Z. Wang, Y.X. Zhang, H.J. Zhao, J. Mater. Chem. A 5 (2017) 23794.
[27] P. Horcajada, T. Chalati, C. Serre, B. Gillet, C. Sebrie, T. Baati, J.F. Eubank, D. Heurtaux, P. Clayette, C. Kreuz, J.S. Chang, Y.K. Hwang, V. Marsaud, P.N. Bories, L. Cynober, S. Gil, G. Ferey, P. Couvreur, R. Gref, Nat. Mater. 9 (2010) 172–178.

[28] S.N. Kim, C.G. Park, B.K. Huh, S.H. Lee, C.H. Min, Y.Y. Lee, Y.K. Kim, K.H. Park, Y.B. Choy, Acta Biomater. 79 (2018) 344–353.
[29] Z.J. Sun, J.Z. Jiang, Y.F. Li, Analyst 140 (2015) 8201–8208.
[30] D.H. Xie, Y. Ma, Y. Gu, H.J. Zhou, H.M. Zhang, G.Z. Wang, Y.X. Zhang, H.J. Zhao, J. Mater. Chem. A 5 (2017) 23794–23804.
[31] Z. Nowroozi-Nejad, B. Bahramian, S. Hosseinkhani, Enzyme Microb. Tech. 121 (2019) 59–67.
[32] W. Liu, W.L. Sun, Y.F. Han, M. Ahmad, J.R. Ni, Colloid. Surface. A 452 (2014) 138–147.
[33] P. Tan, J. Sun, Y.Y. Hu, Z. Fang, Q. Bi, Y.C. Chen, J.H. Cheng, J. Hazard Mater. 297 (2015) 251–260.
[34] A.K. Kushwaha, N. Gupta, M.C. Chattopadhyaya, J. Saudi Chem. Soc. 18 (2014) 200–207.
[35] Y. Xu, J.J. Jin, X.L. Li, Y.D. Han, H. Meng, C.S. Song, X. Zhang, Microchim. Acta 182 (2015) 2313–2320.
[36] M. Hadi, M.R. Samarghandi, G. McKay, Chem. Eng. J. 160 (2010) 408–416.
[37] B.S. Kaith, J. Sharma, S.S. Sukriti, T. Kaur, U. Shanker, V. Jassal, J. Chin. Adv. Mater. Soc. 4 (2016) 249–268.
[38] C. Li, X.J. Wang, D.Y. Meng, L. Zhou, Int. J. Biol. Macrol. 107 (2018) 1871–1878.
[39] R. Jain, S. Sikarwar, Int. J. Environ. Pollut. 27 (2006) 158–178.